Supporting Information

Photoenhanced Interfacial Electron Transfer of Dual Functional Hematite Biophotoelectrode

Chun Hong Mak[a,b], Yong Peng[a,b], Man Hin Chong[a,b], Li Yu[a,b,c], Minshu Du[d], Li Ji[e], Xingli Zou[f], Guizheng Zou[g], Hsin-Hui Shen[*,h], Shella Permatasari Santoso[*,i], Wenxin Niu[j], Fang-Fang Li[k], and Hsien-Yi Hsu[*,a,b]

a. School of Energy and Environment & Department of Materials Science and Engineering & Centre for Functional Photonics (CFP), City University of Hong Kong, Kowloon Tong, Hong Kong, China.

b. Shenzhen Research Institute of City University of Hong Kong, Shenzhen, 518057, China.

c. Key Laboratory for Water Quality and Conservation of the Pearl River Delta, Ministry of Education, Institute of Environmental Research at Greater Bay, Guangzhou University, Guangzhou 510006, China

d. School of Materials Science and Engineering, Northwestern Polytechnical University, Xi'an, Shaanxi 710072, China

e. State Key Laboratory of ASIC and System, School of Microelectronics, Fudan University, Shanghai 200433, China.

f. State Key Laboratory of Advanced Special Steel, School of Materials Science and Engineering, Shanghai University, Shanghai 200072, P. R. China.

g. School of Chemistry and Chemical Engineering, Shandong University, Jinan, 250100, China.

h. Department of Materials Science and Engineering, Faculty of Engineering, Monash University, Clayton, Victoria 3800, Australia

i. Department of Chemical Engineering, Faculty of Engineering, Widya Mandala Surabaya Catholic University, Kalijudan No. 37, Surabaya 60114, East Java, Indonesia;

j. State Key Laboratory of Electroanalytical Chemistry, Changchun Institute of Applied Chemistry, Chinese Academy of Sciences 5625 Renmin Street, Changchun, Jilin 130022, P. R. China

k. School of Materials Science and Engineering, Huazhong University of Science and Technology, 1037 Luoyu Road, Wuhan 430074, China

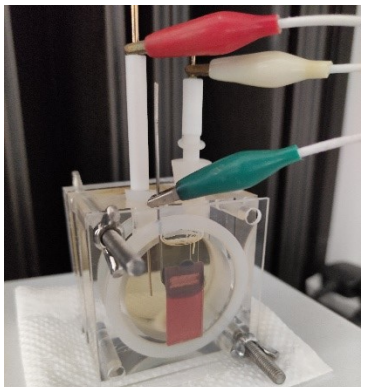

Fig. S1. Assembled S-MPEC chambers Fe_2O_3 as the working electrode.

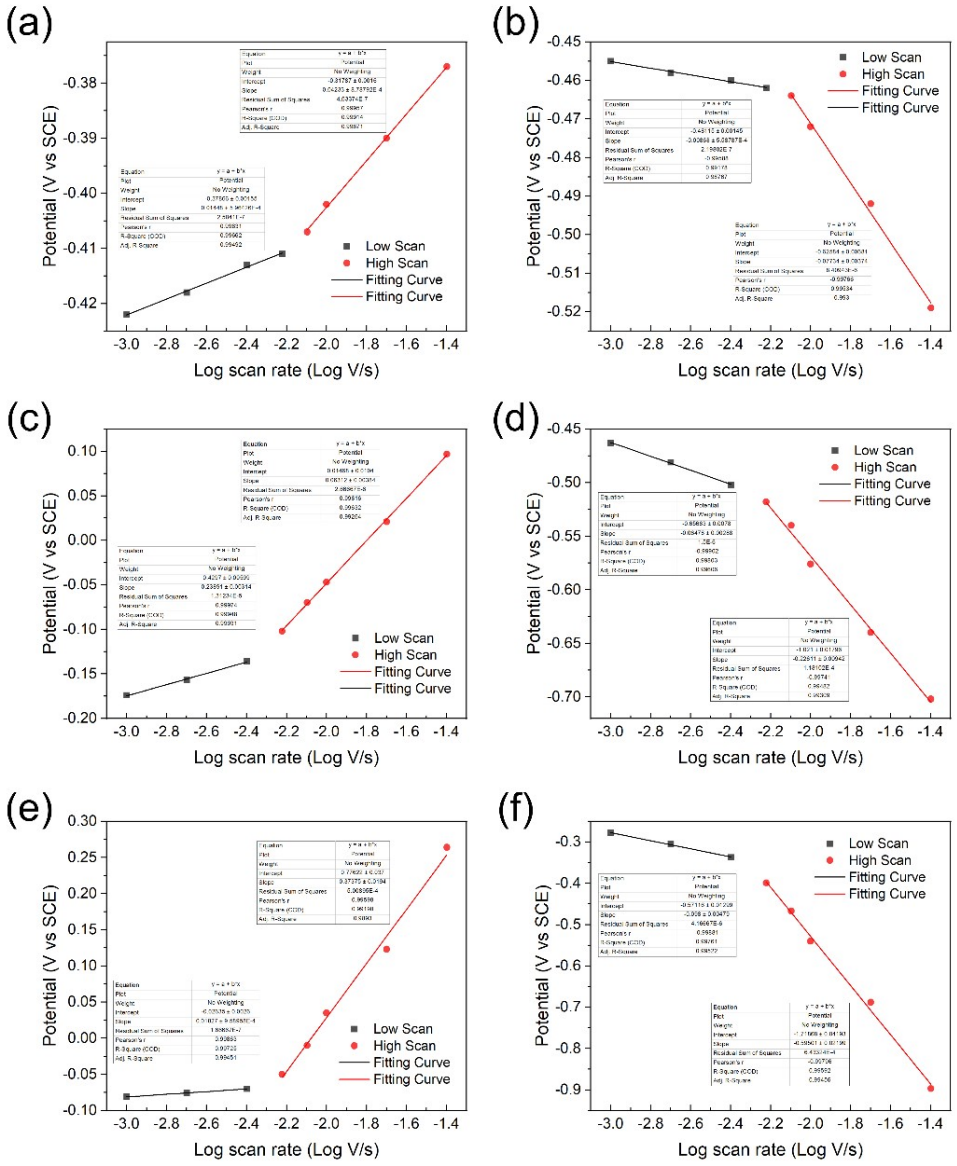

Fig. S2. The plot of E_p against the log of scan rate at low and high scan rates of oxidation reaction using (a) CC-MR-1, (c) Fe_2O_3 and (e) Fe_2O_3-MR-1, as well as reduction reaction using (b) CC-MR-1, (d) Fe_2O_3 and (f) Fe_2O_3-MR-1 to determine of critical scan rate (V_c).

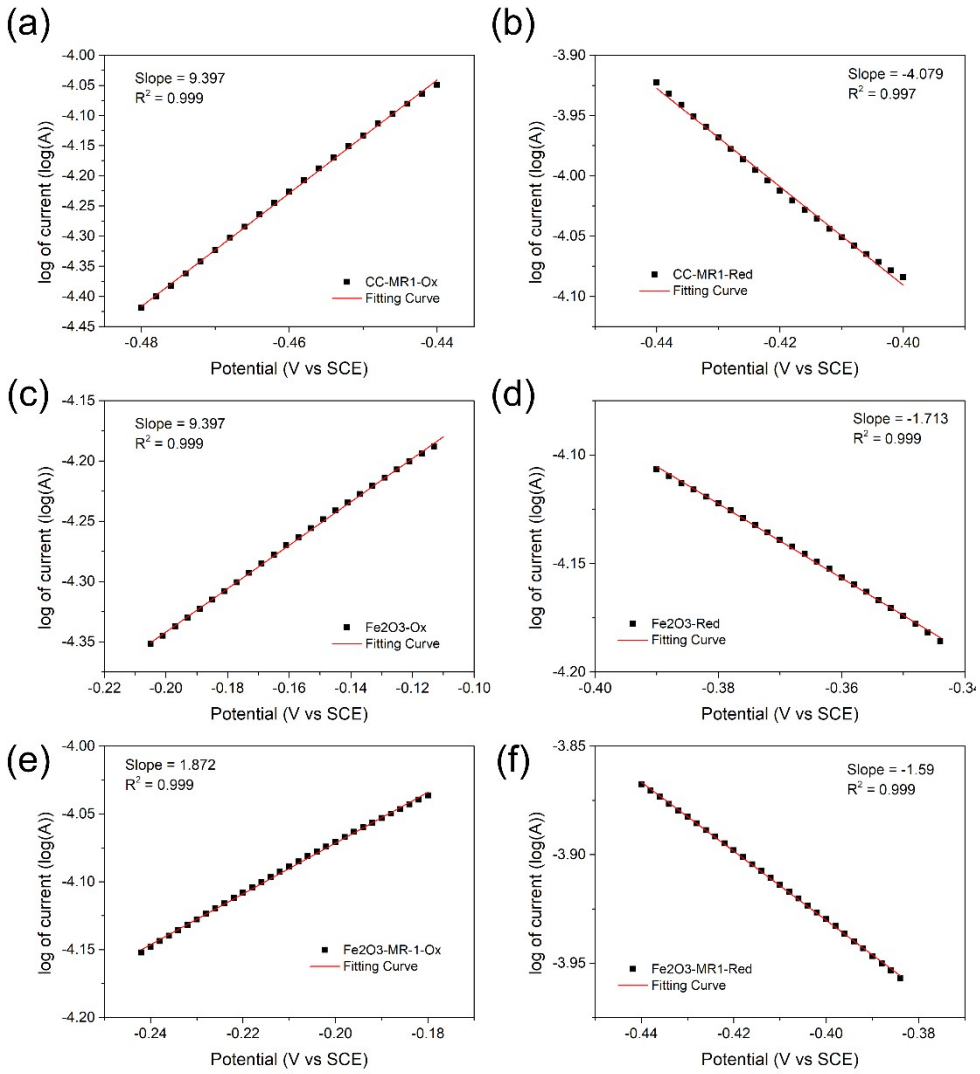

Fig. S3. Tafel plot of the oxidation peak of (a) CC-MR-1, (c) Fe_2O_3 and (e) Fe_2O_3-MR-1 and the reduction peak of (b) CC-MR-1, (d) Fe_2O_3 and (f) Fe_2O_3-MR-1.

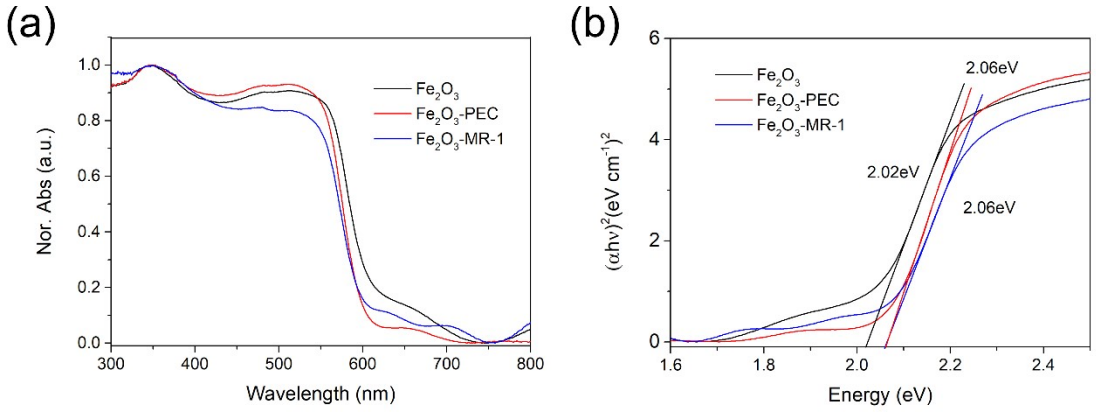

Fig. S4. (a) UV-Vis diffuse reflectance spectrum and (b) Tauc plot of Fe_2O_3, Fe_2O_3 after PEC measurement, and Fe_2O_3-MR-1.

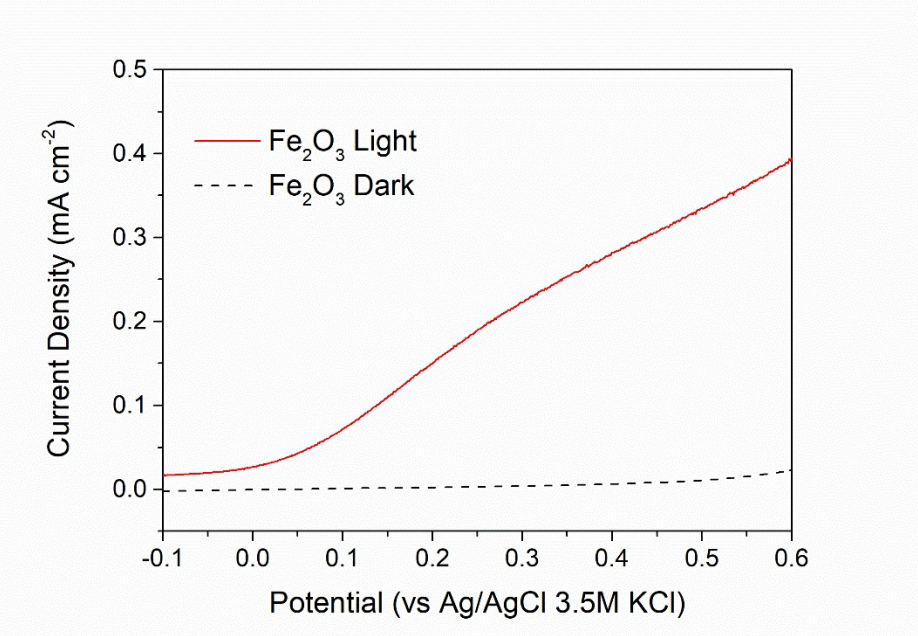

Fig. S5. Linear sweep voltammetry curve of the Fe_2O_3 photoanodes in 1M NaOH under 100 mW cm^{-2} irradiation.

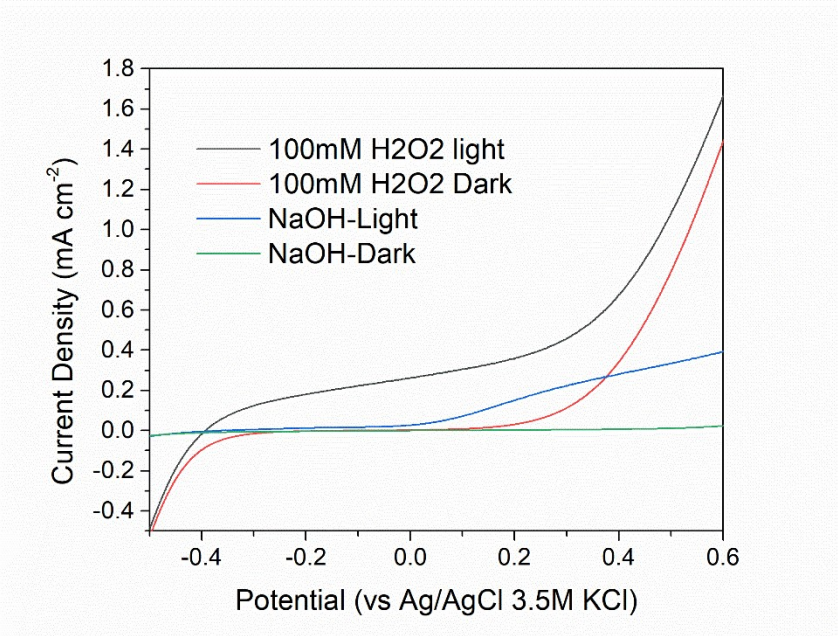

Fig. S6. Linear sweep voltammetry curve of the Fe_2O_3 photoanodes in 1M NaOH with 100mM H_2O_2 as hole scavenger under 100 mW cm^{-2} irradiation.

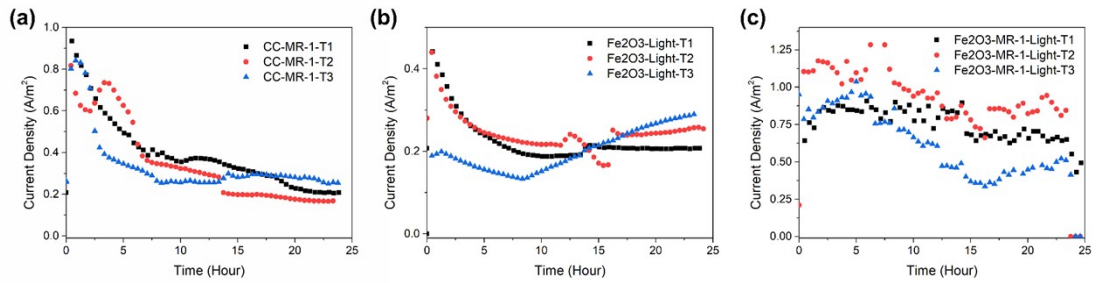

Fig. S7. The I-t curve of the 24-hour operation under the external bias of 0.8V of 3 trials.

Table S1. The Chemical Oxygen Demand (COD) in mg/L of CC-MR-1, Fe_2O_3, Fe_2O_3-MR-1 (dark condition), and Fe_2O_3-MR-1 (irradiated condition) at T0 (0hr), T12 (12hrs), and T24 (24 hrs) under the external bias of 0.8V.

	CC-MR-1	**Fe_2O_3**	**Fe_2O_3-MR-1 (Light)**	**Fe_2O_3-MR-1 (Dark)**
T0 (mg/L)	13,954	14,049	13,932	14,910
T12 (mg/L)	12,654	13,159	12,187	14,143
T24 (mg/L)	12,143	12,579	11,321	13,532
COD removal (mg/L)	1,811	1,470	2,611	1,378

Table S2. Fitted parameters extracted from the Nyquist plots of all prepared sample electrodes.

	CC-MR-1	Bare Fe_2O_3	Fe_2O_3-MR-1
Rs	4.99	143.2	141
CPE1-Anode-T	1.11×10^{-4}	8.95×10^{-9}	2.95×10^{-8}
CPE1-Anode-P	0.5833	1.141	1
Ra	3.769	79.27	75.88
CPE1-Cathode-T	0.00177	5.13×10^{-5}	6.22×10^{-5}
CPE1- Cathode -P	0.742	0.526	0.581
Rc	1007	5967	757.1